0026-895X/96/061495-07$3.00/0

MOLECULAR PHARMACOLOGY, 50:1495–1501 (1996).

Inhibition of Capacitative Ca^{2+} Entry into Cells by Farnesylcysteine Analogs

YAJUN XU, BRYANT A. GILBERT, ROBERT R. RANDO, LONGCHUAN CHEN, and ARMEN H. TASHJIAN, JR.

Department of Molecular and Cellular Toxicology, Harvard School of Public Health (Y.X., L.C., A.H.T.), and the Department of Biological Chemistry and Molecular Pharmacology, Harvard Medical School (B.A.G., R.R.R., A.H.T.), Boston, Massachusetts 02115

Received June 11, 1996; Accepted September 10, 1996

SUMMARY

Capacitative Ca^{2+} influx, which occurs in response to mobilization of intracellular Ca^{2+} stores, is a general feature of many cell types. Although the mechanism of capacitative Ca^{2+} entry is not known, evidence suggests the involvement of small G proteins that are prenylated on a cysteine residue near their carboxyl termini. We have investigated the actions of farnesylcysteine analogs on capacitative Ca^{2+} influx. Using human embryonic kidney 293 cells, we found that *S*-farnesylthioacetic acid, *N*-acetyl-*S*-farnesyl-L-cysteine, *N*-pivaloyl-*S*-farnesyl-L-cysteine, and *N*-acetyl-*S*-gernylgernyl-L-cysteine blocked the activation of capacitative Ca^{2+} influx, whereas *N*-benzoyl-*S*-farnesyl-*S*-cysteine had no effect on capacitative Ca^{2+} entry. Inhibition by *S*-farnesylthioacetic acid was concentration dependent (5–20 μM) and specific for Ca^{2+} influx through nonvoltage-gated Ca^{2+} channels. A single protein band of 26–28 kDa was labeled specifically with a photoaffinity analog of farnesylcysteine. GTP binding to the photoaffinity-labeled band was demonstrated. These findings suggest, but do not prove, that a prenylated substrate, possibly a small G protein, is linked functionally to capacitative Ca^{2+} entry in human embryonic kidney 293 cells.

Capacitative Ca^{2+} influx is a general feature of many cell types that is characterized by entry of extracellular Ca^{2+} after depletion of intracellular Ca^{2+} stores (1, 2). The mechanism by which the content of intracellular stores is coupled to influx of Ca^{2+} across the plasma membrane is unknown. Current hypotheses include direct Ca^{2+} storage vesicle membrane-plasma membrane interactions as well as gating of plasma membrane channels by mediators generated on depletion of intracellular Ca^{2+} stores (2–12).

Fasolato *et al.* (5) and Bird and Putney (13) have presented evidence for involvement of small G proteins in the capacitative Ca^{2+} entry pathway. Rac has been shown to mediate growth factor-induced Ca^{2+} influx (14). Many G proteins, including small G proteins and the γ subunits of heterotrimeric G proteins, are prenylated/methylated at a carboxyl-terminal cysteine residue (15–19). Prenylation has been shown to affect protein-lipid or protein-protein interactions (16, 17).

FC analogs have unique biological actions in different cellular signaling systems. Scheer and Gierschik (20) reported that AFC inhibited receptor-mediated activation of a G protein in isolated membranes. Ding *et al.* (21) demonstrated that specific FC analogs could affect superoxide release in human neutrophils. Ma *et al.* (22) observed that FC analogs blocked platelet aggregation. The mechanism of these actions of FC analogs is not yet fully understood, but they do not seem to be related to effects on methyltransferase activity (21, 22). It is quite possible that they interfere with protein-lipid or protein-protein interactions mediated via prenylated cysteine residues.

SS is an inhibitor of cellular secretion acting via G protein activation, and its receptors are widely distributed in various tissues (23, 24). We have found recently that SSTR2 couples to a pathway that raises $[Ca^{2+}]_i$ in several cell types.[1] When the cDNA for SSTR2 was expressed in HEK 293 cells, a rapid release of intracellular Ca^{2+} was induced by SS (25). Thus, HEK 293 cells expressing the SSTR2 receptor are a useful model to study agonist-induced release of sequestered intra-

This investigation was supported in part by research grants from the National Institutes of Health (DK11011 and NEI03524). Y.X. was supported by National Institutes of Health Training Grant ES07155.

[1] L. Chen and A. H. Tashjian, Jr. Manuscript in preparation.

ABBREVIATIONS: FC, *S*-all-*trans*-farnesyl-L-cysteine; AFC, *N*-acetyl-*S*-farnesyl-L-cysteine; AGGC, *N*-acetyl-*S*-gernylgernyl-L-cysteine; BBB, *N*-α-4-benzoylbenzoyl-L-biocytin; BBB-FC, *N*(*N*-α-4-benzoylbenzoyl-L-biocytin)-*S*-all-*trans*-farnesyl-L-cysteine; $[Ca^{2+}]_i$, cytosolic free calcium concentration; EGTA, ethylene glycol bis(β-aminoethyl ether)-*N*,*N*,*N*′,*N*′-tetraacetic acid; FTA, *S*-farnesylthioacetic acid; HBSS, Hanks' balanced salt solution; HEPES, *N*-2-hydroxyethyl-piperazine-*N*′-2-ethanesulfonic acid; PFC, *N*-pivaloyl-*S*-farnesyl-L-cysteine; SDS, sodium dodecyl sulfate; PAGE, polyacrylamide gel electrophoresis; SS, somatostatin; SSTR2, somatostatin receptor subtype 2; Tg, thapsigargin; HEK; human embryonic kidney; SMS, somatostatin analog SMS201-995 (octreotide).

cellular Ca^{2+} and the subsequent Ca^{2+} depletion-initiated Ca^{2+} influx pathway.

We report herein that several FC analogs block capacitative Ca^{2+} entry in SSTR2-transfected HEK 293 cells. These analogs specifically inhibited capacitative Ca^{2+} entry through a non-voltage-dependent Ca^{2+} influx pathway. The inhibitory mechanism is different from that of other known blockers of capacitative Ca^{2+} influx, such as SK&F 96365 (26, 27) and carboxy-amido-triazole (28, 29), which inhibit both voltage-gated and non-voltage-operated Ca^{2+} influx. Therefore, these FC analogs should prove useful as new reagents to investigate the biochemical mechanisms of capacitative Ca^{2+} entry.

Materials and Methods

Fura-2 acetoxymethyl ester was obtained from Molecular Probes (Eugene, OR). Tg was obtained from Calbiochem (San Diego, CA). Culture media and sera for cell culture were purchased from GIBCO (Grand Island, NY). Other chemicals were obtained from Sigma Chemical (St. Louis, MO). [^{125}I]Tyr^{11}-somatostatin (2000 Ci/mmol) and [α-^{32}P]GTP (2300 Ci/mmol) were obtained from Amersham (Arlington Heights, IL). Immobilized monomeric avidin-agarose was purchased from Pierce Chemical (Rockford, IL). Avidin-conjugated horseradish peroxidase and prestained and biotinylated molecular-weight markers were from BioRad (Hercules, CA). The luminal chemiluminescence Western blotting detection reagents were purchased from Amersham Life Science (Clearbrook, IL).

HEK 293 cells stably expressing SSTR2. HEK 293 cells (American Type Culture Collection, Rockville, MD) were transfected stably with the cDNA for SSTR2. A cDNA clone of mouse SSTR2A in the plasmid PCMV6C (provided by Dr. Graeme I. Bell, Department of Biochemistry and Molecular Biology, University of Chicago, Chicago, IL) was cotransfected into HEK 293 cells with pcDNAIneo using the lipofectin method according to manufacturer's protocol (GIBCO/BRL, Gaithersburg, MD). Transfected cells were selected with 500 μg/ml G418 and individual colonies were isolated. SSTR2 receptor positive clones were identified by ^{125}I-Tyr^{11}-somatostatin binding assays (30).

Cell culture. HEK 293 cells were cultured as monolayers at 37° in Eagle's minimum essential medium supplemented with 10% (v/v) fetal bovine serum in a humidified atmosphere of 95% air/5% CO_2. Rat pituitary GH_4C_1 cells (31) were grown in Ham's F10 medium supplemented with 15% horse serum and 2.5% fetal bovine serum.

Measurement of $[Ca^{2+}]_i$. All measurements were performed in Fura-2-loaded cells. Cells were harvested in HEPES-buffered HBSS-II (118 mM NaCl, 4.6 mM KCl, 10 mM D-glucose, 20 mM HEPES, pH 7.2) containing 0.02% EDTA. The cell suspension was washed once with HBSS-I (1 mM $CaCl_2$, 118 mM NaCl, 4.6 mM KCl, 10 mM D-glucose, 20 mM HEPES, pH 7.2), and cells were loaded with Fura-2 acetoxymethyl ester (50–100 μM) for 30 min at 37°. The cells were then washed twice with HBSS-I and resuspended in the same buffer. Fluorescence measurements of the cell suspension were performed at 30° with constant stirring using a Spex Fluorolog FIIIA spectrophotofluorometer (Spex Industries, Edison, NJ) at an excitation wavelength of 342 nm and an emission wavelength of 492 nm. $[Ca^{2+}]_i$ was calculated using the equation: $[Ca^{2+}]_i = K_d (F - F_{min})/(F_{max} - F)$, where K_d is 224 nM (32) and F is the fluorescence signal in arbitrary units. F_{max} (maximum fluorescence) was obtained by permeabilizing the cells with 25 μM digitonin in the presence of 1 mM $CaCl_2$, and F_{min} (minimum fluorescence) was obtained by chelating calcium with 5 mM EGTA [pH adjusted to 8.3 with 1 M Tris base].

Mn^{2+} entry was measured using a Hitachi F-2000 Spectrofluorimeter (Hitachi, Yokohama, Japan). Fluorescence emission at 500 nm was obtained after dual wavelength excitation at 340 and 360 nm.

Cell extract preparation. Whole-cell homogenates and soluble cell fractions were prepared as described previously (33).

Measurement of protein. Protein concentration was determined by the BioRad method, according to the manufacturer's protocol.

FC analogs. BBB was prepared according to the published procedure (34). The syntheses of FC methyl ester (35), AFC (36), FTA (36), PFC (21, 22), and AGGC (36) have been reported previously. The conditions used for photolysis, SDS-PAGE, and Western blotting of BBB-FC-photolabeled HEK 293 cell homogenates (see below) were identical to those reported for the photoaffinity labeling and detection of aspartic proteases (34).

Proton NMR (^{1}H NMR) spectroscopy was obtained with a Varian VRX 500S Spectrometer (San Fernando, CA) operating at a proton frequency of 499.843 MHz. Dimethylsulfoxide-d_6 was used as the ^{1}H NMR solvent. The residual proton absorption of the deuterated solvent was used as the internal standard. All ^{1}H NMR chemical shifts are reported as d values in ppm, and the coupling constants (J) are given in Hertz. Mass spectra were obtained on a Finnigan 4000 mass spectrometer (San Jose, CA).

Synthesis of BBB-FC. 1-Ethyl-2-(2-dimethylaminopropyl)carbodiimide (19 mg, 0.10 mmol) was added in one portion to a solution of BBB (52 mg, 0.089 mmol), FC methyl ester (38 mg, 0.11 mmol), and 1-hydroxybenzotriazol hydrate (15 mg, 0.11 mmol) in dimethylformamide (2 ml). The mixture was stirred at 0° for 2 hr and then stored overnight at room temperature. The reaction was quenched with 3.5% aqueous HCl (10 ml), and the solution was extracted with n-butanol (3 × 25 ml). The combined organic layers were washed with brine (2 × 20 ml), dried over $MgSO_4$, filtered, and concentrated to give a white solid. The material was purified by silica gel chromatography (5% methanol in Dulbecco's culture medium) to obtain the methyl ester as a white crystalline solid in 73% yield: thin layer chromatography R_F = 0.43 (5% methanol in Dulbecco's culture medium); [^{1}H NMR (dimethylsulfoxide-d_6) δ 8.58 (1 H, d, J = 7.9 Hz), 8.43 (1 H, d, J = 7.5 Hz), 8.02 (2 H, d, J = 8.9 Hz), 7.78 (1 H, d, J = 8.9 Hz), 7.74–7.67 (6 H, m), 7.56 (2 H, t, J = 7.9 Hz), 6.37 (1 H, s), 6.31 (1 H, s), 5.12 (1 H, t, J = 7.5 Hz), 5.03 (2 H, br s), 4.51–4.41 (2 H, m), 4.26 (1 H, t, J = 5.5 Hz), 4.08 (1 H, t, J = 5.5 Hz), 3.61 (3 H, s), 3.20–2.95 (7 H, m), 2.84–2.66 (4 H, m), 2.53 (1 H, d, J = 12Hz), 2.06–1.94 (8 H, m), 1.88 (1 H, t, J = 7.5 Hz), 1.79–1.68 (2 H, m), 1.48–1.20 (10 H, m), 1.59 (3 H, s), 1.58 (3H, s), 1.51 (3 H, s)]; fast-atom bombardment, high-resolution mass spectrometry (nitrobenzyl acid) m/z 924.4380 $(M+Na)^+$, $C_{49}H_{67}N_5O_7S_2$ requires 901.

The corresponding carboxylic acid of BBB-FC was obtained by saponification of its methyl ester with 10% aqueous KOH in methanol (5.0 ml) according to the published procedure (34). The NMR spectra of the acid was essentially identical to the methyl ester, except that the singlet resonance at d 3.61 ppm was absent.

Photoaffinity labeling of HEK 293 cell homogenates. Total homogenates of HEK 293 cells (0.2 mg of protein) were incubated for 10 min at room temperature in a final volume of 200 μl containing 20 μM BBB-FC. FTA or other additions were made to the final concentrations indicated in the figure legends. The sample tubes were incubated in ice-cold water and photolyzed with strong light (350 nm) for 15 min. Samples that were not subjected to photolysis were treated identically and used as controls for nonspecific labeling. After photolysis, 30 μl of 100% trichloroacetic acid was added to each sample (final concentration, 15%) and kept on ice for 10 min. The protein precipitates were collected by centrifugation for 10 min and washed three times with 500 μl of ice-cold acetone to remove residual trichloroacetic acid. The pellets were resuspended in 100 μl of 2× Laemmli/SDS sample buffer (37) and boiled for 15 min before analysis by SDS-PAGE (12%) (37). The gels were transblotted onto a nitrocellulose membrane, and biotinylated proteins were identified with horseradish peroxidase-linked streptavidin and detected by chemiluminescence.

Streptavidin fractionation of photoaffinity-labeled HEK 293 cell homogenates. The soluble fraction of HEK 293 cell homogenates was photolyzed as described above. After photolysis, 30 ml of streptavidin-linked agarose beads (Pierce Chemical) was added and mixed at 4° for 30 min. Samples were pelleted and the beads were

washed twice with 0.5 ml of phosphate-buffered solution (1× = 10 mM Na_2HPO_4, pH 7.4, 150 mM NaCl). The beads were then suspended in 50 μl of Laemmli/SDS sample buffer and boiled for 20 min. The samples were centrifuged and the supernatant solutions were analyzed by SDS-PAGE. The gels were transblotted onto a nitrocellulose membrane and analyzed by chemiluminescence (as described above) and for GTP binding.

GTP binding. The transfer blots from the streptavidin fractionation were incubated in buffer (50 mM Tris-Cl, pH 7.5, 5 mM $MgCl_2$, 2 mM dithiothreitol, 0.3% Tween 20, 0.3% bovine serum albumin, 0.1 mM ATP) with shaking at room temperature for 1 hr. The blot was then transferred to buffer containing [α-^{32}P]GTP (1 mCi/ml; specific activity, 2300 Ci/mmol) with shaking at room temperature for 1 hr. The blot was washed three times with buffer and [α-^{32}P]GTP binding was detected by autoradiography.

Results

Inhibition of capacitative Ca^{2+} influx by FTA. HEK 293 cells stably expressing SSTR2 were loaded with Fura-2 and challenged with a supermaximal concentration (100 nM) of the somatostatin receptor agonist, SMS 201–995 (Octreotide), in the presence of 1 mM extracellular Ca^{2+}. A biphasic elevation of $[Ca^{2+}]_i$ was observed, consisting of a transient peak followed by a sustained plateau above the basal $[Ca^{2+}]_i$ (Fig. 1A). When EGTA was added to chelate extracellular Ca^{2+}, the elevated plateau phase of $[Ca^{2+}]_i$ fell to below the base-line (Fig. 1A). When SMS 201–995 was added to cells in Ca^{2+}-free buffer, the transient spike in $[Ca^{2+}]_i$ was still elicited but the plateau phase of rise in $[Ca^{2+}]_i$ was eliminated (Fig. 1B), indicating that the second phase of Ca^{2+} elevation (presumably capacitative Ca^{2+} entry; see below) was dependent on influx of extracellular Ca^{2+}. Furthermore, if intracellular Ca^{2+} pools were depleted by prior incubation with Tg, SS no longer elicited entry of extracellular Ca^{2+}, indicating that the plateau phase of Ca^{2+} influx was capacitative. When FTA (10 μM) was added before (Fig. 1C) or after (Fig. 1D) addition of SMS, the plateau phase of rise in $[Ca^{2+}]_i$ was eliminated, indicating that FTA inhibited receptor-activated entry of extracellular Ca^{2+}. It should be noted that FTA alone can induce a small increase in $[Ca^{2+}]_i$ (Fig. 1, C and F), which is dependent on extracellular Ca^{2+} (data not shown). The mechanism of this small FTA-induced Ca^{2+} influx is unknown at present.

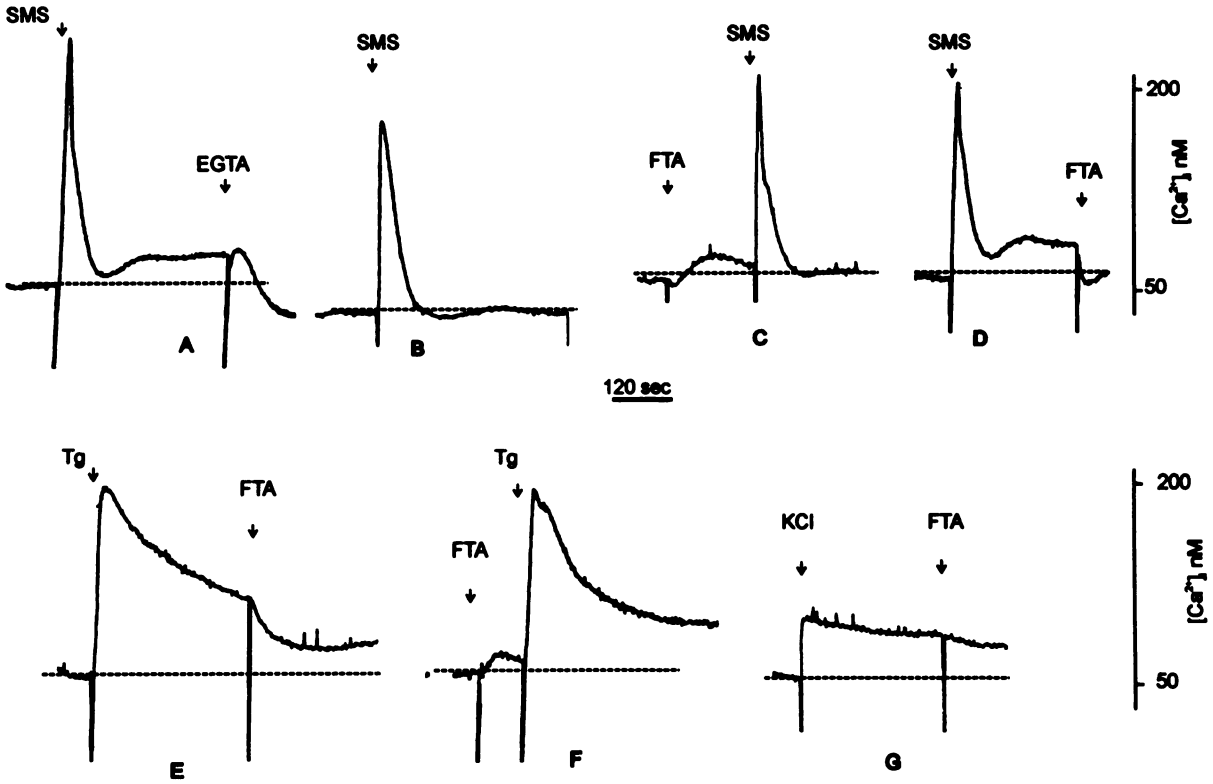

Fig. 1. Actions of FTA on SS- and Tg-induced Ca^{2+} influx. A through F, results with HEK 293 cells. G, results with GH_4C_1 cells. HEK 293 cells stably expressing the SSTR2 receptor (A through F) were loaded with Fura-2 in HBSS-I buffer and washed with HBSS-I buffer (except in B, in which cells were washed with HBSS Ca^{2+}-free buffer) before measurements of $[Ca^{2+}]_i$. The SS agonist octreotide (SMS, 100 nM) was added to induce Ca^{2+} release from intracellular stores (the initial large peak in $[Ca^{2+}]_i$). A, After establishment of the second phase of rise in $[Ca^{2+}]_i$, due to influx of extracellular Ca^{2+}, addition of 5 mM EGTA caused a rapid fall in $[Ca^{2+}]_i$. B, In Ca^{2+}-free buffer, addition of SMS (100 nM) elicited only the acute rise in $[Ca^{2+}]_i$ due to release of intracellular Ca^{2+}. There was no secondary plateau because there was no free extracellular Ca^{2+} available to enter the cells. C, When FTA (10 μM) was added before SMS, the secondary phase of rise in $[Ca^{2+}]_i$ was blocked. D, When FTA (10 μM) was added after establishment of SMS-induced Ca^{2+} entry, it terminated that process. E, Release of intracellular Ca^{2+} stores was induced by Tg (1 μM). The peak phase was followed by a gradual decline in $[Ca^{2+}]_i$, which is the balance between extrusion of Ca^{2+} from the cell and depletion-induced entry of extracellular Ca^{2+}. When FTA (10 μM) was added, there was a decrease in $[Ca^{2+}]_i$ due to diminished entry of extracellular Ca^{2+}. F, When FTA (10 μM) was added before the Tg (1 μM), the rate of fall of $[Ca^{2+}]_i$ from the Tg-induced peak was greater than in cells treated with Tg alone (E). G, Rat pituitary GH_4C_1 cells, which have voltage-gated Ca^{2+} channels, were loaded with Fura-2 and washed with Ca^{2+}-containing HBSS-I buffer. Addition of 30 mM KCl caused entry of extracellular Ca^{2+} (not observed in Ca^{2+}-free buffer) and a rise in $[Ca^{2+}]_i$, which was not affected by subsequent addition of 10 μM FTA. Addition of FTA before KCl did not block depolarization-induced entry of extracellular Ca^{2+} in GH_4C_1 cells (data not shown).

Tg, an inhibitor of the ATPase that loads inositol(1,4,5)-trisphosphate-sensitive Ca^{2+} stores, induces capacitative Ca^{2+} entry in cells due to depletion of certain intracellular Ca^{2+} storage compartments (1). When HEK 293 cells were incubated with Tg (1 μM), a prolonged elevation of $[Ca^{2+}]_i$ was observed (Fig. 1E). In the absence of extracellular Ca^{2+} or after addition of EGTA, the Tg-induced rise in $[Ca^{2+}]_i$ fell rapidly toward base-line (not shown), indicating that the prolonged phase of elevation of $[Ca^{2+}]_i$ was due to entry of extracellular Ca^{2+}. Addition of FTA, after Tg, decreased Ca^{2+} entry (Fig. 1E). If FTA was added before Tg, the half-time of decay of the Tg-induced fluorescence maximum (Fig. 1F) was decreased from 220 ± 15 sec to 105 ± 15 sec (mean ± standard error of five experiments).

Inhibition of Tg-induced Ca^{2+} entry by FTA was concentration dependent. In Ca^{2+}-free HBSS buffer, Tg elicited a rapid rise and a rapid decrease in $[Ca^{2+}]_i$ (Fig. 2). Addition of 1 mM Ca^{2+} caused rapid Ca^{2+} influx, and preaddition of FTA inhibited this Ca^{2+} influx in a concentration-dependent manner (Fig. 2). Because HEK 293 cells do not have voltage-operated L-type Ca^{2+} channels (no Ca^{2+} influx is induced by 50 mM extracellular K^+), inhibition by FTA of Ca^{2+} influx in these cells must occur via another channel or pathway. To test directly whether FTA could inhibit influx of Ca^{2+} through voltage-operated Ca^{2+} channels, we examined the action of FTA on high K^+-induced Ca^{2+} entry in another cell type, GH_4C_1 rat pituitary cells, which have well-characterized L-type Ca^{2+} channels (38–40). Even at high concentrations, FTA (50 μM) did not inhibit Ca^{2+} influx induced by KCl in GH_4C_1 cells (Fig. 1G). This result also demonstrates that FTA does not act by chelating Ca^{2+} or as a nonspecific Ca^{2+} entry blocker.

Inhibition by FTA of Tg-stimulated entry of extracellular Mn^{2+}. We used an additional approach to demonstrate depletion-induced divalent cation influx by measuring Mn^{2+} entry into Fura-2-loaded HEK 293 cells. When Mn^{2+} binds to Fura-2, the fluorescence of the probe is quenched (41). Thus, Mn^{2+}, which can enter cells via certain Ca^{2+} influx pathways, can be used as a surrogate for Ca^{2+} (41). Fura-2 was excited at two wavelengths (340 and 360 nm) to allow simultaneous monitoring of changes in $[Ca^{2+}]_i$ and quenching of fluorescence by Mn^{2+}. The data in Fig. 3 show the emission at 492 nm from Fura-2-loaded HEK 293 cells. The increase in $[Ca^{2+}]_i$ induced by Tg was indicated by the peak in fluorescence excited at 340 nm (F_{340}) (Fig. 3A). There was a small decrease in fluorescence excited at 360 nm (F_{360}). When extracellular Mn^{2+} was added, it entered the cells rapidly and quenched fluorescence excited at both wavelengths (Fig. 3B). When FTA (20 μM) was added before addition of extracellular Mn^{2+}, there was attenuation in the rate of Mn^{2+} entry as monitored by the decrease in fluorescence excited at both wavelengths (Fig. 3A). The initial rate of Mn^{2+}-induced fluorescence quenching, in cells pretreated with Tg and then FTA, decreased to 30 ± 10% (mean ± standard error of six independent measurements) of the rate observed in cells pretreated with Tg alone (Fig. 3A versus Fig. 3C). The rate of fluorescence quenching by Mn^{2+} in control cells (not pretreated with Tg) was similar to that observed in cells pretreated with both Tg and FTA (see Fig. 3B versus Fig. 3A), indicating that FTA inhibited depletion-induced Mn^{2+} (and so Ca^{2+}) entry essentially to basal control levels.

Actions of several FC analogs on Ca^{2+} influx. Because FTA is a potent inhibitor of both bovine and human methyltransferases (22), we tested other FC analogs (methyltransferase substrates as well as inhibitors) to determine whether inhibition of depletion-induced Ca^{2+} influx could be explained by inhibition of methyltransferase activity. The results shown in Fig. 4 indicate that AFC (Fig. 4A) and AGGC (Fig. 4C), which are substrates for methyltransferase (22), inhibited Tg-induced Ca^{2+} influx. PFC, which is neither a substrate nor an inhibitor of methyltransferase, inhibited Ca^{2+} influx modestly (Fig. 4B), and *N*-benzoyl-FC, which is also neither a substrate nor an inhibitor, had no effect on Ca^{2+} influx, even at a concentration of 200 μM. Importantly, *S*-adenosyl-L-homocysteine, which is a potent inhibitor (K_i = 1.6 μM) of methyltransferase (21), had no effect on Ca^{2+} influx at a concentration of 50 μM (data not shown). Because PFC could inhibit Ca^{2+} influx, whereas it does not bind to the methyltransferase (19), and because *S*-adenosyl-L-homocysteine had no effect on Ca^{2+} influx, although it is a potent inhibitor of methyltransferase, we conclude that the inhibitory actions of the FC analogs FTA, AFC, AGGC, and PFC on

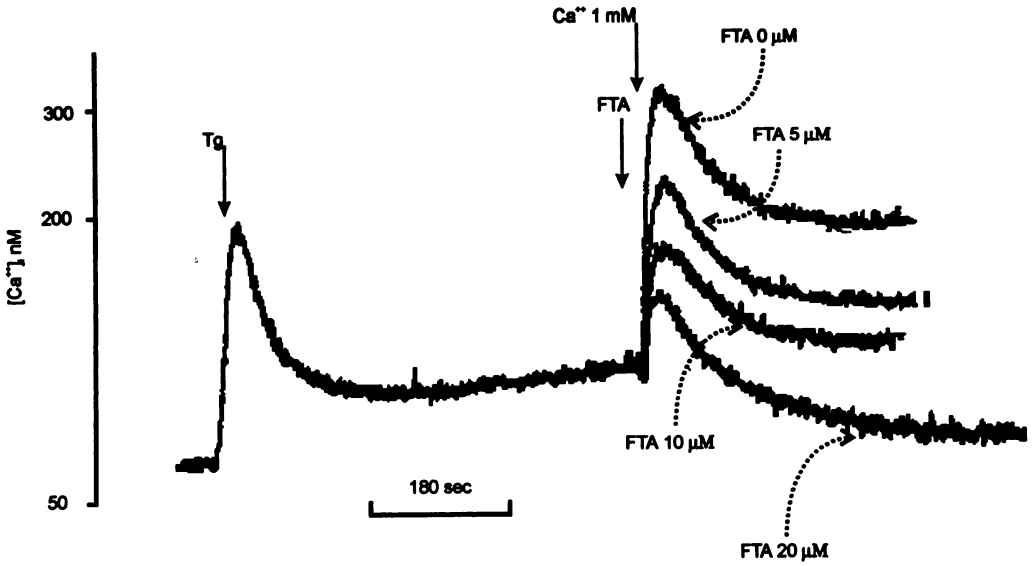

Fig. 2. Concentration-dependent inhibition by FTA of Tg-induced entry of extracellular Ca^{2+}. HEK 293 cells were loaded with Fura-2 and suspended in Ca^{2+}-free HBSS-II buffer. Tg (1 μM) was added to release intracellular Ca^{2+} stores, and after about 10 min, 1 mM Ca^{2+} was added to the buffer to initiate Ca^{2+} influx (FTA = 0 mM). Addition of increasing concentrations of FTA (5–20 μM) were made just before the Ca^{2+} addition, as shown by the *arrow* marked FTA.

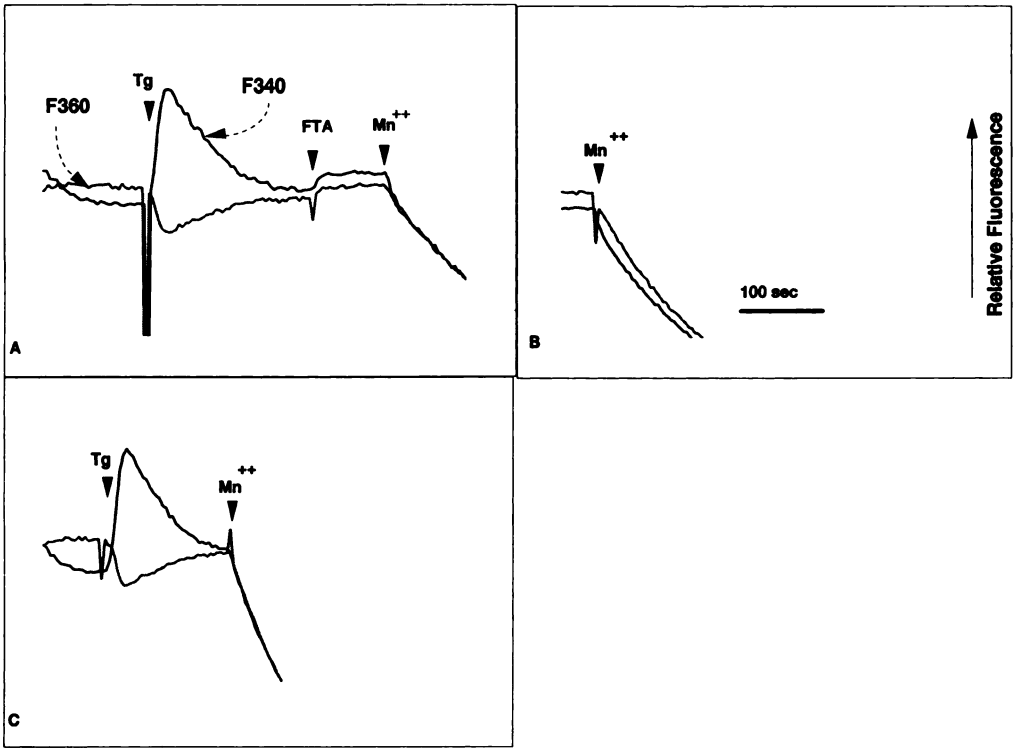

Fig. 3. Action of FTA on depletion-induced entry of extracellular Mn^{2+}. HEK 293 cells were loaded with Fura-2 and resuspended in Ca^{2+}-free HBSS-II buffer. Fluorescence emission was monitored at 492 nm after excitation at 340 or 360 nm. A, Tg (1 μM) was added about 3.3 min before addition of FTA (20 μM) and subsequent addition of $MnCl_2$ (250 μM). B, $MnCl_2$ (250 μM) was added to untreated control cells. C, Tg (1 μM) was added about 2.5 min before addition of $MnCl_2$ (250 μM). FTA reduced the rate of Mn^{2+} entry induced by Tg to about the basal rate of Mn^{2+} influx (see A and B compared with C). The time line in B applies to all three panels.

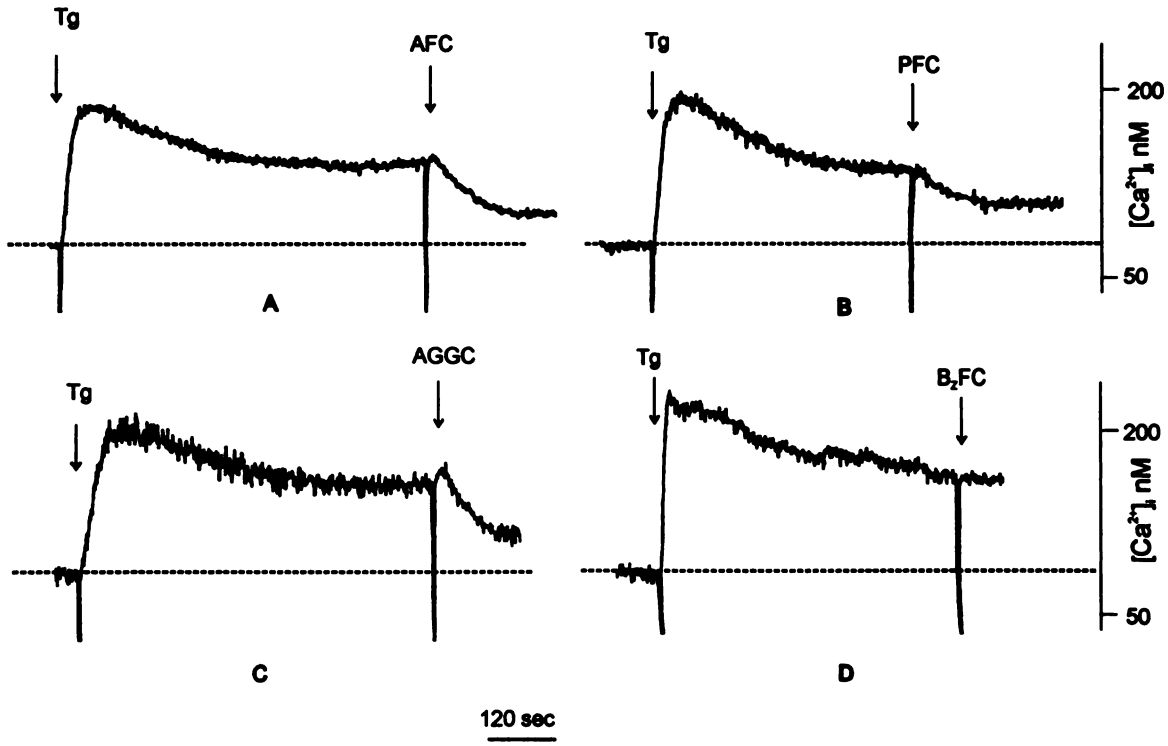

Fig. 4. Actions of several FC analogs on Tg-induced Ca^{2+} influx. HEK 293 cells were incubated with Tg (1 μM), and then the individual FC analogs were added separately and the effects on $[Ca^{2+}]_i$ were monitored. A, 50 μM AFC. B, 50 μM PFC. C, 10 μM AGGC. D, 200 μM *N*-benzoyl-FC (*B_2FC*).

Ca^{2+} influx induced by Tg are not likely to be explained by inhibition of methyltransferase activity.

Photoaffinity labeling of HEK 293 cell homogenates with an FTA photoprobe. To begin to investigate the target of FTA action, we used a benzophenone derivative of biotinylated FTA (BBB-FC). Whole homogenates of HEK 293 cells were incubated with BBB-FC in the absence or presence of excess FTA for 10 min at room temperature. The samples were then photolyzed for 15 min at 0°. After SDS-PAGE, the biotinylated proteins were identified with horseradish peroxidase-linked streptavidin using chemiluminescence. After photolysis, a band of 26–28 kDa was prominently labeled

(Fig. 5, *lane 2*, *arrowhead*). This band was not detected in the unphotolyzed control sample (Fig. 5, *lane 1*) and labeling was completely blocked by added FTA (Fig. 5, *lane 3*).

GTP binding. Streptavidin beads were used to isolate biotinylated proteins after photoaffinity labeling. These proteins were separated on SDS-PAGE and the gel was transblotted. The blot was analyzed by chemiluminescence and for [^{32}P]GTP binding. A single band of about 26–28 kDa was detected by chemiluminescence only in the sample that was irradiated with light in the absence of added FTA (Fig. 6, *lane 2*). Labeled GTP binding was superimposed on the 26–28-kDa band (Fig. 6, *lane 5*). GTP binding was not detected in streptavidin-isolated unirradiated samples or in samples photolyzed in the presence of added FTA.

The photoaffinity labeling of a single 26–28-kDa band with an FTA photoprobe and the binding of GTP to this same band suggest a selective interaction of FTA with a molecule that can also bind GTP. This dually labeled band has the size characteristics of a small G protein. However, our data do not prove that the FTA target is, in fact, a G protein or that the labeled band is a functional target for inhibition of capacitative Ca^{2+} entry by FTA. Nevertheless, together with previous data that a small G protein is involved in capacitative Ca^{2+} entry (5, 13, 14), our findings with a new class of Ca^{2+} depletion-induced Ca^{2+} entry inhibitors suggest that this hypothesis should be pursued further.

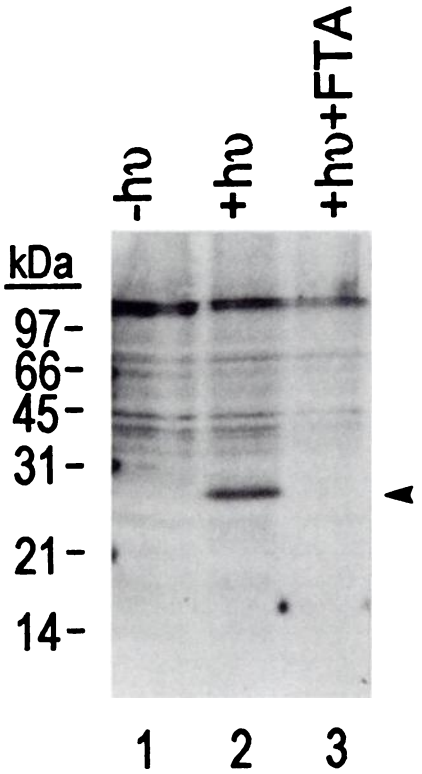

Fig. 5. Photoaffinity labeling of HEK 293 cell homogenates with an FTA probe. HEK 293 cell homogenates (0.2 mg of protein) were photoaffinity labeled with BBB-FC, and the labeled proteins were resolved on a 12% SDS-PAGE gel, blot transferred, and detected by chemiluminescence (see Materials and Methods). *Lane 1*, incubation with 20 μM BBB-FC without irradiation (−hν). *Lane 2*, incubation with 20 μM BBB-FC with irradiation (+hν). *Lane 3*, incubation with 20 μM BBB-FC plus 1 mM FTA with irradiation (+hν + FTA). *Arrowhead*, specifically labeled band with a molecular mass of 26–28 kDa.

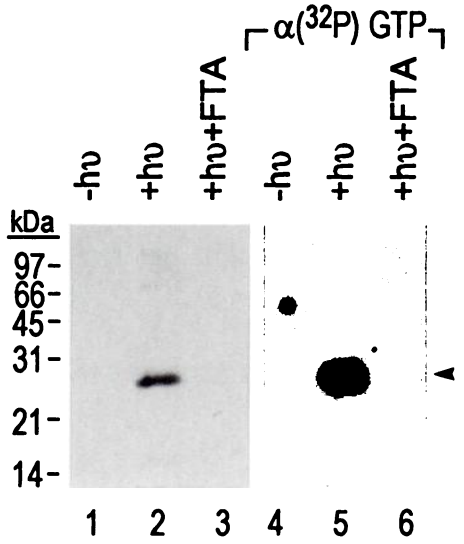

Fig. 6. Isolation of photoaffinity-labeled HEK 293 cell products and GTP binding. HEK 293 cell homogenates were photoaffinity labeled as described in Materials and Methods and mixed with streptavidin beads. Biotinylated products that bound to the beads were released by boiling in sample buffer and were separated on a 12% SDS-PAGE gel, blot transferred, and analyzed by chemiluminescence (*lanes 1–3*) and for [^{32}P]GTP binding (*lanes 4–6*). *Lanes 1 and 4*, incubation with 20 μM BBB-FC without irradiation (−hν). *Lanes 2 and 5*, incubation with 20 μM BBB-FC with irradiation (+hν). *Lanes 3 and 6*, incubation with 20 μM BBB-FC plus 1 mM FTA with irradiation (+hν + FTA). *Arrowhead*, specifically labeled band with a molecular mass of 26–28 kDa.

Discussion

Results presented in this report demonstrate that FTA and certain other FC analogs inhibit capacitative Ca^{2+} influx induced either by agonist action or release of intracellular Ca^{2+} stores by Tg. These inhibitors acted on a non-voltage-gated Ca^{2+} influx pathway. It is known that Ca^{2+} entry through Ca^{2+}-release activated Ca^{2+} channels is sensitive to membrane potential. Therefore, we examined the action of FTA at depolarizing concentrations of extracellular K^+ (30 mM) and found that FTA inhibited Mn^{2+} entry induced by Tg to the same extent as observed in low K^+ (4.6 mM) buffer (data not shown). The Ca^{2+} entry-inhibiting activity of FC analogs is not related to possible activities as substrates or inhibitors of methyltransferase because FC analogs inert with respect to methyltransferase were active here. To probe the possible cellular targets of FTA action, we performed affinity-labeling experiments with a photoactivatable derivative of FC. A single band with a molecular weight of 26–28 kDa was specifically labeled, and this band also had GTP binding activity. Although we have not demonstrated that this band contains the cellular target of FTA action on Ca^{2+} influx, it has the size and nucleotide binding characteristics of the small G protein family of transducing factors. Because only a single band of 26–28 kDa was labeled with the FTA photoaffinity probe in the crude whole-cell homogenate, it is unlikely that FTA interacts directly with the Ca^{2+}-release activated Ca^{2+} channel to block Ca^{2+} entry.

How a small G protein might act to mediate capacitative Ca^{2+} influx is not known (5, 13). However, prenylation is known to be important for the interaction of several small G proteins with the cell membrane components (15, 16), for example, interaction of the stimulatory and inhibitory GDP/GTP exchange proteins and their effector proteins (16, 42), possibly via preny-

lated protein-protein or protein-lipid interactions. Small G proteins play a role in several signal transduction pathways, including depletion-induced Ca^{2+} entry (1, 13, 43). For example, Rac has been shown to be involved in Ca^{2+} influx induced by growth factors (14). Rac is also a mediator of superoxide release in human neutrophils. We speculate that Rac or another small G protein may be involved functionally in capacitative Ca^{2+} influx, and FC analogs could act to interfere with prenylated protein-lipid or prenylated protein-protein interactions to antagonize this influx pathway. However, until the specific molecular target of FTA (or other FC analogs) is identified, the precise mechanism of action of these agents to inhibit depletion-induced Ca^{2+} entry remains speculative. Nevertheless, these FC analogs should prove to be useful probes for elucidating the biochemical mechanism or mechanisms of capacitative Ca^{2+} entry.

Acknowledgments

We thank Younghee Lim for her technical help and Jean Foley for her assistance in the preparation of the manuscript.

References

1. Putney, J. W., Jr. Capacitative calcium entry revisited. *Cell Calcium* **11**:611–624 (1990).
2. Randriamampita, C., and R. Y. Tsien. Emptying of intracellular Ca^{2+} stores releases a novel small messenger that stimulates Ca^{2+} influx. *Nature (Lond.)* **364**:809–814 (1993).
3. Irvine, R. F. Inositol phosphates and Ca^{2+} entry: toward a proliferation or a simplification? *FASEB J.* **6**:3085–3091 (1992).
4. Fasolato, C., B. Innocenti, and T. Pozzan. Receptor-activated Ca^{2+} influx: how many mechanisms for how many channels? *Trends Pharmacol. Sci.* **15**:77–83 (1994).
5. Fasolato, C., M. Hoth, and R. Penner. A GTP-dependent step in the activation mechanism of capacitative calcium influx. *J. Biol. Chem.* **268**: 20737–20740 (1993).
6. Berridge, M. J. Inositol trisphosphate and calcium signalling. *Nature (Lond.)* **361**:315–325 (1993).
7. Parekh, A. B., H. Terlau, and W. Stuhmer. Depletion of $InsP_3$ stores activates a Ca^{2+} and K^+ current by means of a phosphatase and a diffusible messenger. *Nature (Lond.)* **364**:814–818 (1993).
8. Montero, M., J. Garcia-Sancho, and J. Alvarez. Activation by chemotactic peptide of a receptor-operated Ca^{2+} entry pathway in differentiated HL60 cells. *J. Biol. Chem.* **269**:29451–29456 (1994).
9. Xu, X., R. A. Star, G. Tortorici, and S. Muallem. Depletion of intracellular Ca^{2+} stores activates nitric-oxide synthase to generate cGMP and regulate Ca^{2+} influx. *J. Biol. Chem.* **269**:12645–12653 (1994).
10. Vostal, J. G., W. L. Jackson, and N. R. Shulman. Cytosolic and stored calcium antagonistically control tyrosine phosphorylation of specific platelet proteins. *J. Biol. Chem.* **266**:16911–16916 (1991).
11. Lee, K.-M., K. Toscas, and M. L. Villereal. Inhibition of bradykinin- and thapsigargin-induced Ca^{2+} entry by tyrosine kinase inhibitors. *J. Biol. Chem.* **268**:9945–9948 (1993).
12. Ufret-Vincenty, C. A., A. D. Short, A. Alfonso, and D. L. Gill. A novel Ca^{2+} entry mechanism is turned on during growth arrest induced by Ca^{2+} pool depletion. *J. Biol. Chem.* **270**:26790–26793 (1995).
13. Bird, G. St. J., and J. W. Putney, Jr. Inhibition of thapsigargin-induced calcium entry by microinjected guanine nucleotide analogues. Evidence for the involvement of a small G-protein in capacitative calcium entry. *J. Biol. Chem.* **268**:21486–21488 (1993).
14. Peppelenbosch, M. P., L. G. J. Tertoolen, A. M. M. de Vries-Smits, R.-G. Qiu, L. M'Rabet, M. H. Symons, S. W. de Laat, and J. L. Bos. Rac-dependent and -independent pathways mediate growth factor-induced Ca^{2+} influx. *J. Biol. Chem.* **271**:7883–7886 (1996).
15. Casey, P. J., J. F. Moomaw, F. L. Zhang, J. B. Higgins, and J. A. Thissen. Prenylation and G protein signaling. *Recent Prog. Horm. Res.* **49**:215–238 (1994).
16. Ando, S., K. Kaibuchi, T. Sasaki, K. Hiraoka, T. Nishiyama, T. Mizuno, M. Asada, H. Nunoi, I. Matsuda, Y. Matsuura, P. Polakis, F. McCormick, and Y. Takai. Post-translational processing of rac p21s is important both for their interaction with the GDP/GTP exchange proteins and for their activation of NADPH oxidase. *J. Biol. Chem.* **267**:25709–25713 (1992).
17. McGeady, P., S. Kuroda, K. Shimizu, Y. Takai, and M. H. Gelb. The farnesyl group of h-ras facilitates the activation of a soluble upstream activator of mitogen-activated protein kinase. *J. Biol. Chem.* **270**:26347–26351 (1995).
18. Sinensky, M., and R. J. Lutz. The prenylation of proteins. *Bioessays* **14**:25–31 (1992).
19. Ma, Y.-T., and R. R. Rando. A microsomal endoprotease that specifically cleaves isoprenylated peptides. *Proc. Natl. Acad. Sci. USA* **89**:6275–6279 (1992).
20. Scheer, A., and P. Gierschik. Farnesylcysteine analogues inhibit chemotactic peptide receptor-mediated G-protein activation in human HL-60 granulocyte membranes. *FEBS Lett.* **319**:110–114 (1993).
21. Ding, J., D. J. Lu, D. Perez-Sala, Y.-T. Ma, J. F. Maddox, B. A. Gilbert, J. A. Badwey, and R. R. Rando. Farnesyl-L-cysteine analogs can inhibit or initiate superoxide release by human neutrophils. *J. Biol. Chem.* **269**: 16837–16844 (1994).
22. Ma, Y.-T., Y. Q. Shi, Y. H. Lim, S. H. McGrail, J. A. Ware, and R. R. Rando. Mechanistic studies on human platelet isoprenylated protein methyltransferase: farnesylcysteine analogs block platelet aggregation without inhibiting the methyltransferase. *Biochemistry* **33**:5414–5420 (1994).
23. Reichlin, S. Somatostatin (first of two parts). *N. Engl. J. Med.* **309**:1495–1501 (1983).
24. Reichlin, S. Somatostatin (second of two parts). *N. Engl. J. Med.* **309**:1556–1563 (1983).
25. Chen, L., and A. H. Tashjian, Jr. Somatostatin acting via the SSTR2 receptor subtype, increases $[Ca^{2+}]_i$ in addition to inhibiting adenylate cyclase, in *Proceedings of the 76th Annual Meeting of the Endocrine Society*, Endocrine Society Press, Bethesda, MD, 589 (1994).
26. Gusovsky, F., J. E. Lueders, E. C. Kohn, and C. C. Felder. Muscarinic receptor-mediated tyrosine phosphorylation of phospholipase C-gamma. An alternative mechanism for cholinergic-induced phosphoinositide breakdown. *J. Biol. Chem.* **268**:7768–7772 (1993).
27. Merritt, J. E., W. P. Armstrong, C. D. Benham, T. J. Hallam, R. Jacob, A. Jaxa-Chamiec, B. K. Leigh, S. A. McCarthy, K. E. Moores, and T. J. Rink. SK&F 96365, a novel inhibitor of receptor-mediated calcium entry. *Biochem. J.* **271**:515–522 (1990).
28. Felder, C. C., A. L. Ma, L. A. Liotta, and E. C. Kohn. The antiproliferative and antimetastatic compound L651582 inhibits muscarinic acetylcholine receptor-stimulated calcium influx and arachidonic acid release. *J. Pharmacol. Exp. Ther.* **257**:967–971 (1991).
29. Hupe, D. J., R. Boltz, C. J. Cohen, J. Felix, E. Ham, D. Miller, D. Soderman, and D. Van Skiver. The inhibition of receptor-mediated and voltage-dependent calcium entry by the antiproliferative L-651,582. *J. Biol. Chem.* **266**:10136–10142 (1991).
30. Bruno, J. F., Y. Xu, J. Song, and M. Berelowitz. Molecular cloning and functional expression of a brain-specific somatostatin receptor. *Proc. Natl. Acad. Sci. USA* **89**:11151–11155 (1992).
31. Tashjian, A. H., Jr. Clonal strains of hormone-producing pituitary cells. *Methods Enzymol.* **58**:527–535 (1979).
32. Grynkiewicz, G., M. Poenie, and R. Y. Tsien. A new generation of Ca^{2+} indicators with greatly improved fluorescence properties. *J. Biol. Chem.* **260**:3440–3450 (1985).
33. Brady, K. D., B. Han, and A. H. Tashjian, Jr. Kinetics and reversibility of thyrotropin-releasing hormone-stimulated guanine nucleotide exchange in membranes from GH_4C_1 cells. *Mol. Pharmacol.* **46**:644–652 (1994).
34. Gilbert, B. A., and R. R. Rando. Modular design of biotinylated photoaffinity probes — synthesis and utilization of a biotinylated pepstatin photoprobe. *J. Am. Chem. Soc.* **117**:8061–8066 (1995).
35. Brown, M. J., P. D. Milano, D. C. Lever, W. W. Epstein, and C. D. Poulter. Prenylated proteins. A convenient synthesis of farnesyl cysteinyl thioethers. *J. Am. Chem. Soc.* **113**:3176–3177 (1991).
36. Gilbert, B. A., E. W. Tan, D. Perez-Sala, and R. R. Rando. Structure-activity studies on the retinal rod outer segment isoprenylated protein methyltransferase. *J. Am. Chem. Soc.* **114**:3966–3973 (1992).
37. Laemmli, U. K. Cleavage of structural proteins during the assembly of the head of bacteriophage T4. *Nature (Lond.)* **227**:680–685 (1970).
38. Tan, K.-N., and A. H. Tashjian, Jr. Voltage-dependent calcium channels in pituitary cells in culture. I. Characterization by $^{45}Ca^{2+}$ fluxes. *J. Biol. Chem.* **259**:418–426 (1984).
39. Albert, P. R., and A. H. Tashjian, Jr. Thyrotropin-releasing hormone-induced spike and plateau in cytosolic free Ca^{2+} concentrations in pituitary cells. Relation to prolactin release. *J. Biol. Chem.* **259**:5827–5832 (1984).
40. Tornquist, K., and A. H. Tashjian, Jr. Dual actions of 1,25-dihydroxycholecalciferol on intracellular Ca^{2+} in GH_4C_1 cells: evidence for effects on voltage-operated Ca^{2+} channels and Na^+/Ca^{2+} exchange. *Endocrinology* **124**:2765–2776 (1989).
41. Hallam, T. J., and T. J. Rink. Agonists stimulate divalent cation channels in the plasma membrane of human platelets. *FEBS Lett.* **186**:175–179 (1985).
42. Hori, Y., A. Kikuchi, M. Isomura, M. Katayama, Y. Miura, H. Fujioka, K. Kaibuchi, and Y. Takai. Post-translational modifications of the C-terminal region of the rho protein are important for its interaction with membranes and the stimulatory and inhibitory GDP/GTP exchange proteins. *Oncogene* **6**:515–522 (1991).
43. Hall, A. Small GTP-binding proteins and the regulation of the actin cytoskeleton. *Annu. Rev. Cell Biol.* **10**:31–54 (1994).

Send reprint requests to: Dr. Armen H. Tashjian, Jr., Department of Molecular and Cellular Toxicology, Harvard School of Public Health, 665 Huntington Avenue, Boston, MA 02115. E-mail: tashjian@hsph.harvard.edu